

Article

Wild Plant Habitat Characterization in the Last Two Decades in the Nile Delta Coastal Region of Egypt

Ahmed El-Zeiny ^{1,*}, Shrouk A. Elagami ², Hoda Nour-Eldin ³, El-Sayed F. El-Halawany ², Giuliano Bonanomi ⁴, Ahmed M. Abd-ElGawad ⁵, Walid Soufan ⁵ and Yasser A. El-Amier ^{2,*}

¹ Environmental Studies Department, National Authority for Remote Sensing and Space Sciences (NARSS), Cairo 11769, Egypt

² Department of Botany, Faculty of Science, Mansoura University, Mansoura 35516, Egypt; shrouk_elagami@outlook.com (S.A.E.); drelhalawany@mans.edu.eg (E.-S.F.E.-H.)

³ Land Use Department, National Authority for Remote Sensing and Space Sciences (NARSS), Cairo 11769, Egypt; hoda.noureldin@narss.sci.eg

⁴ Department of Agriculture, University of Naples Federico II, 80055 Naples, Italy; giuliano.bonanomi@unina.it

⁵ Plant Production Department, College of Food and Agriculture Sciences, King Saud University, P.O. Box 2460, Riyadh 11451, Saudi Arabia; aibrahim2@ksu.edu.sa (A.M.A.-E.); wsoufan@ksu.edu.sa (W.S.)

* Correspondence: aelzeny@narss.sci.eg (A.E.-Z.); yasran@mans.edu.eg (Y.A.E.-A.); Tel.: +20-100-773-7052 (A.E.-Z.); +20-101-722-9120 (Y.A.E.-A.)



Citation: El-Zeiny, A.; Elagami, S.A.; Nour-Eldin, H.; El-Halawany, E.-S.F.; Bonanomi, G.; Abd-ElGawad, A.M.; Soufan, W.; El-Amier, Y.A. Wild Plant Habitat Characterization in the Last Two Decades in the Nile Delta Coastal Region of Egypt. *Agriculture* **2022**, *12*, 108. <https://doi.org/10.3390/agriculture12010108>

Academic Editor: Belen Franch

Received: 30 November 2021

Accepted: 10 January 2022

Published: 13 January 2022

Publisher's Note: MDPI stays neutral with regard to jurisdictional claims in published maps and institutional affiliations.



Copyright: © 2022 by the authors. Licensee MDPI, Basel, Switzerland. This article is an open access article distributed under the terms and conditions of the Creative Commons Attribution (CC BY) license (<https://creativecommons.org/licenses/by/4.0/>).

Abstract: Environmental and land-use changes put severe pressure on wild plant habitats. The present study aims to assess the biodiversity of wild plant habitats and the associated spatiotemporal environmental changes in the coastal region of Dakahlia Governorate following an integrated approach of remote sensing, GIS, and samples analysis. Thirty-seven stands were spatially identified and studied to represent the different habitats of wild plants in the Deltaic Mediterranean coastline region. Physical and chemical characteristics of soil samples were examined, while TWINSpan classification was used to identify plant communities. Two free Landsat images (TM and OLI) acquired in 1999 and 2019 were processed to assess changes via the production of land use and cover maps (LULC). Moreover, NDSI, NDMI, and NDSI indices were used to identify wild plant habitats. The floristic composition indicated the existence of 57 species, belonging to 51 genera of 20 families. The largest families were *Asteraceae*, *Poaceae*, and *Chenopodiaceae*. The classification of vegetation led to the identification of four groups. Canonical Correspondence Analysis (CCA) revealed that electrical conductivity, cations, organic carbon, porosity, chlorides, and bicarbonates are the most effective soil variables influencing vegetation. The results of the spectral analysis indicated an annual coverage of bare lands (3.56 km²), which is strongly related to the annual increase in vegetation (1.91 km²), water bodies (1.22 km²), and urban areas (0.43 km²). The expansion of urban and agricultural regions subsequently increased water bodies and caused occupancy of bare land, resulting in the development of wild plant habitats, which are mostly represented by the sparse vegetation class as evaluated by NDVI. The increase in mean moisture values (NDMI) from 0.03 in 1999 to 0.15 in 2019 might be explained by the increase in total areas of wild plant habitats throughout the study period (1999–2019). This may improve the adequacy of environments for wild habitats, causing natural plant proliferation.

Keywords: coastal habitats; wild plants; remote sensing; GIS; vegetation dynamics

1. Introduction

Habitat destruction is one of the major threats facing plant species conservation throughout the world. In the Nile Delta, urban crawling and seawater intrusion are the primary threat to the survival of wildlife [1]. When an ecosystem has been dramatically altered by human activities such as agriculture, oil and gas exploration, commercial development, or water diversion it may no longer be able to provide the food, water, cover, and places to

raise young that wildlife needs to survive [2,3]. Egypt's coasts run for almost 3500 km along the Mediterranean Sea, Red Sea, and Sinai Peninsula. Egypt's Mediterranean coastline region has a narrow coastal strip that stretches for roughly 970 km from Sallum (on the Libyan border) eastward to Rafah (on the Palestinian border), with an average width of 20–25 km from north to south. [4]. In Egypt's coastal zones, unplanned development, land subsidence, high erosion rates, waterlogging, saltwater intrusion, soil salinization, and ecosystem degradation are all major concerns.

Coastal areas are typically rich in natural resources, which provide excellent opportunities for economic activities, particularly resource-based economic activities such as agriculture, fisheries, tourism, oil and gas extraction, and maritime transportation, which all tend to be concentrated in these areas. Furthermore, coastal locations serve as important gathering points for a huge number of immigrants, with rising need for housing, energy, products, and services [5,6]. The flora of the Nile Delta coastal land is rich in many wild plant species, which seem to be economically promising. The Deltaic Mediterranean coast is distinguished into two divisions: (1) The coastal zone, which can be subdivided into sand dunes, sand flats, salt marshes, and sandy fertile lands; (2) The shorelines of the north-eastern corner of Lake Manzala [4]. On the other hand, the cultivated land habitats can be divided into: (1) Winter crops, comprising clover, wheat, broad beans, flax, and winter vegetables; (2) Summer crops, comprising rice, cotton, maize, and summer vegetables; and (3) Orchards, comprising citrus, grapes, and bananas.

Monitoring habitat quality, according to Zlinszky et al. [7], necessitates a complex integration of numerous ecosystem variables, while standard terrestrial data-gathering methods have shown to be time-consuming and difficult to evaluate owing to inter-subjective variations. Furthermore, many important ecosystems are inaccessible. These issues need the development of systems that can swiftly and accurately provide repeatable outcomes on very large sizes [8,9]. Change detection research on native ecosystems is critical, as our metropolitan centers' native plant diversity is rapidly dwindling. Such investigations may now be carried out without the need for personal involvement by using appropriate digital image-processing techniques on multispectral images [10–12]. Integrating GIS and RS (Remote Sensing) have evolved into powerful tools for variables acquisition and environmental vulnerability spatial distribution studies [13,14]. Normalized Difference Vegetation Index (NDVI) is highly correlated with parameters associated with plant health and productivity, such as vegetation density and cover [15,16], green leaf biomass [17], leaf area index [18], chlorophyll content [19], crop condition [20], and wild plant habitat [10,11].

As a result, the current study attempts to assess habitat characteristics in the coastal region of Dakahlia Governorate, as well as to conduct a comparative assessment of frequently used spectral indices for accuracy and applicability with Landsat 8 OLI and TM pictures. In addition, the study aims to establish a field survey and investigate innovative approaches for delivering current and accurate information on the location of wild plant habitats in the coastal region of the Dakahlia Governorate. The presence and vitality of the vegetation were identified using NDVI (Normalized Difference Vegetation Index) temporal patterns generated from a series of geometrically registered and radiometrically calibrated TM and OLI Landsat images spanning the years 1999 to 2019. Moreover, two factors influencing the environment along the Mediterranean coast impacted the NDVI: soil salinity NDSI (Normalized Difference Salinity Index) and waterlogging NDMI (Normalized Difference Moisture Index).

2. Materials and Methods

2.1. Study Area

The Mediterranean coastal area of the Dakahlia Governorate is located between latitude $30^{\circ}35'10''$ to $31^{\circ}34'02''$ N and longitude $31^{\circ}12'47''$ to $32^{\circ}07'25''$ E, covering 3985.76 km² of the Nile Delta region of Egypt [21]. According to a map showing the geographical distribution of dry regions [22], the Nile Delta's climatic conditions are similar to those of northern Egypt; it is arid-to-semi-arid, with evaporation rates several times higher than

precipitation rates. Ayyad and Floc'h [23] recognized that the Mediterranean coastal region lies in an attenuated arid province characterized by short dry periods, annual rainfall, warm summers, and mild winters. As a result, Dakahlia Governorate, which is part of the Deltaic Mediterranean coast, falls under the dry and/or semi-arid climatic zones of Egypt's northern shoreline region [24]. The sampling stands were selected according to certain distribution to cover all physiographic variations in each habitat and to ensure sampling of a wide range of vegetation variations. The total number of stands was 37 samples from the coastal region of Dakahlia Governorate, as shown in Figure 1, and their details are described in Supplementary Materials Table S1.

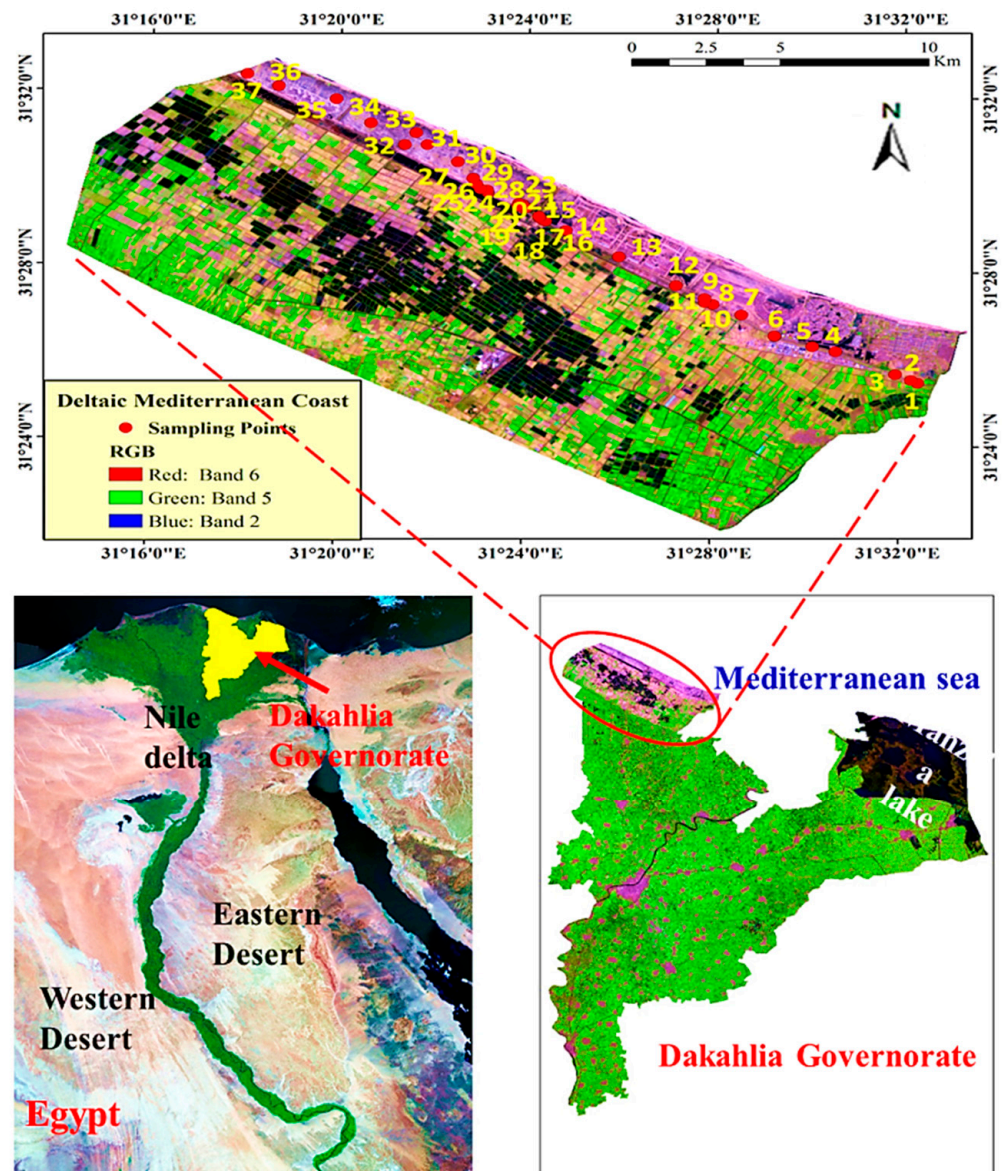


Figure 1. Map of Egypt showing Dakahlia Governorate and location of the studied sites (1–37) along the Nile Delta coast (Dakahlia Governorate).

The meteorological conditions on Egypt's Deltaic Mediterranean coast are dry-to-semi-arid, with evaporation rates many times higher than precipitation rates [23] and temperatures in the hottest months of the summer reaching 30 °C on average. On the other hand, the mean monthly temperature value in the winter is above 10 °C. Although the climate of the Nile Delta coast is not so different from the climate of the western and eastern Mediterranean sections, its vegetation is different because of physicochemical properties of

soil, presence of three natural lakes, and anthropogenic activities. Moreover, it is affected not only by seawater but also by the leakage water from the River Nile branches (Damietta and Rosetta branches), as well as the northern lakes [4].

2.2. Vegetation Analysis

Six field trips were conducted during the period 19 March–5 May 2019. During this period, 37 stands were selected randomly along the Mediterranean coastline (Dakahlia Governorate) to cover all physiographic variations in each habitat and to ensure sampling of a wide range of vegetation variations. Three quadrates (20 × 20 m each) were conducted in each stand, and the density and cover of each species were visually evaluated. Shukla and Chandel [25] were used to determine the density of each plant species; meanwhile, Canfield [26] was used to determine the plant cover of each species in the studied stands. For each plant species, relative values of density and cover were computed and averaged to generate an estimate of its importance value (IV) in each quadrate, which was then pooled for each stand. The taxonomic nomenclature, identification, and chorotype of plant species were assessed according to Boulos [27], Boulos [28], Boulos [29], and Täckholm [30]. Life forms, on the other hand, were recognized using Raunkjær [31] approach.

2.3. Soil Analysis

Within each quadrate, a georeferenced soil sample was collected and the three soil samples of the three quadrates were pooled as composite samples. The soil samples were packed in polyethylene bags and returned to the laboratory for further analysis. The samples were allowed to air-dry at room temperature, before being sieved through a 2 mm sieve to remove the roots and coarse debris, and then sealed in bags until further physical and chemical analysis. Piper [32] was used to measure soil particle size, water-holding capacity (WHC), organic carbon, and sulfate. Chlorides and calcium carbonate content, in addition to soil pH and electrical conductivity (EC), were measured in water suspension (1:2.5) as described by Jackson [33]. Titration with 0.1 N HCl was used to measure carbonates and bicarbonates [34]. According to McKell and Goodin [35], the extractable cations Na⁺ and K⁺ were evaluated using flame photometry (PHF 80B Biologie Spectrophotometer), whereas Ca⁺² and Mg⁺² were calculated using an atomic absorption spectrometer (A Perkin-Elmer, Model 2380, Wellesley, MA, USA).

2.4. Spectral Analysis

2.4.1. Satellite Image Acquisition and Preprocessing

Two free Landsat downloadable images of the sensors TM and OLI 8 acquired on the 6th of March 1999 and 19th of March 2019 were used. The study area was covered by two different scenes (i.e., path 176, rows 38 and 39) as row data (i.e., digital number; DN). Radiometric Calibration and Atmospheric Correction were applied on the Landsat images to eliminate atmospheric effects using ENVI V5.3. The study area was cropped from the georeferenced mosaic using a shape file of the Governorate administrative boundary.

2.4.2. Image Processing

To bring out visual features, image processing was used to transform and alter the original raw data [36]. ENVI 5.3 was used to build LULC maps using supervised classification using the maximum likelihood classifier (MLC). According to Table 1, three indices were calculated: NDVI, NDSI, and NDMI. In two years, LULC and spectral indices maps were used to track environmental changes in the research region (1999 and 2019). Field validation visits were planned to ensure that the classification was accurate.

Table 1. Spectral indices formula and classes used in the present study.

Index	Formula	Classes (Ranges)	References
Normalized Difference Vegetation Index (NDVI)	$NDVI = \frac{(NIR-Red)}{(NIR+Red)}$	−1–0.25 No vegetation 0.25–0.5 Sparse vegetation 0.5–0.75 Moderate vegetation 0.75–1 Dense vegetation	[37,38]
Normalized Difference Salinity Index (NDSI)	$NDSI = \frac{(Red-NIR)}{(Red+NIR)}$	−1–0 Non saline 0–0.25 Slightly saline 0.25–0.5 Moderately saline 0.5–1 Highly saline	[39]
Normalized Difference Moisture Index (NDMI)	$NDMI = \frac{(NIR-SWIR)}{(NIR+SWIR)}$	NDMI > 0.1 High humidity NDMI < 0.1 Low humidity	[37]

2.4.3. Post-Classification Techniques

Post-classification comparisons of the retrieved thematic maps were used for simple change detection and for quantifying various types of change using ArcGIS 10.5. The degree of success and accuracy depends on the reliability of the resulting classification maps [40]. In a GIS environment, the classification raster maps were turned into thematic layers to facilitate examining temporal and geographical changes and the yearly rate of rise and decline among various classes. Statistics, including maximum, minimum, and the mean values for NDVI, NDMI, and NDSI were determined to detect the changes that occurred over the last two decades.

2.5. Data Analysis

The Community Analysis Package (version 1.2, Pisces Conservation Ltd., Lymington, UK, <http://www.pisces-conservation.com/softcap.html>, 30 May 1999) application was used to perform cluster analysis (two-way indicator species analysis, TWINSpan) and ordination (detrended correspondence analysis, DCA) of stands according to Hill and Šmilauer [41]. However, Canonical Correspondence Analysis (CCA) was performed using the MVSP Program (version 3.2, Kovach Computing Services, Wales, UK, <https://www.kovcomp.co.uk/index.html>, 15 October 2021) [42]. Using the COSTAT 6.3 program (CoHort Software, Monterey, CA, USA, <http://www.cohort.com>, 1 April 2005), the soil variables for each community were submitted to one-way ANOVA and the mean values were separated based on Duncan's test at the 0.05 probability level.

3. Results and Discussion

3.1. Floristic Composition

The floristic diversity of the study area includes 57 species (34 annual, 1 biennial, and 22 perennial species) through 37 sites in the north sector of Nile Delta (Dakahlia Governorate), belonging to 51 genera and 20 families. The sampling was carried during the rainy season. The wet season gives a greater opportunity for a large number of annuals to bloom. Asteraceae, Poaceae, and Chenopodiaceae had the most species (11, 13, and 6, respectively), while Brassicaceae and Caryophyllaceae had four species, each. Fabaceae, Aizoaceae, and Polygonaceae had three, two, and two species, respectively. These families constituted 78.95% of the documented species and represent most of the floristic structure in the study area, while the other 12 families were monospecific and shared 21.05% of the listed species. The wide ecological range of Asteraceae and Poaceae can be attributed to their adaptation to harsh conditions, as well as their effective dispersal of seeds or spores by the wind [43]. Plant species that belong to the Poaceae have some characteristics that allow them to tolerate grazing pressure and drought, and even profit from it. They have developed a dense surface root system that allows them to absorb moisture from the soil effectively [44]. The Asteraceae family is the largest and has the most widely distributed blooming plant species in the world [45,46]; however, it is not the only major family in Egypt's flora [28,30,47].

Based on the presence percentage, the recorded species were categorized into three main classes: (1) Wide-range distribution class (presence > 50%), represented with five plant species, namely *Senecio glaucus* (86.49%), *Rumex pictus* (78.38%), *Ifloga spicata* (70.27%), *Calligonum polygnooides* (62.16%), and *Lotus halophilus* (51.35%); (2) Moderate distribution class (presence ranges from 50–25%), which encompasses 10 species, including *Poa annua* (45.95%), *Silene vivianii* (43.24%), *Cutandia memphitica* (37.84%), *Mesembryanthemum nodiflorum* (37.84%), and *Echinopus spinosus* (37.84%); (3) Narrow-range distribution class (presence < 25%), which made up the remaining 42 species, including *Carthamus tenuis* (18.92%), *Chenopodium mural* (16.22%), *Lolium multiflorum* (13.51%), *Melilotus indicus* (8.11%), and *Pancratium maritimum* (2.70%) (Supplementary Materials Table S2).

Therophytes made up the majority of the species found in this study (59.32%), followed by geophytes (11.86%), then hemicryptophytes (10.17%), nanophanerophytes (8.47%), and chamaephytes (6.78%) (Supplementary Materials Table S2). Therophytes' dominance over other life forms appears to be a reaction to the hot, dry environment, topographical changes, and human and animal disturbance [48–50]. They are adapted to the region's dryness and lack of rainfall because they spend their vegetative life as seeds [51,52]. These findings are consistent with the plant spectrum found in arid environments throughout the Middle East [53,54].

3.2. Chorological Affinities

Egypt is a crossroads for floristic components from at least four phytogeographical regions: African Sudano-Zambian, Asiatic Irano-Turanian, Afro-Asian Saharo-Sindian, and Euro-Afro-Asian Mediterranean [55]. The Saharo-Arabian zone of the Holarctic floristic region encompasses the whole nation. According to a chorological study of the surveyed flora, 39 species (68.42%) were pluri-, bi-, or mono-regional Mediterranean components (Supplementary Materials Table S3). Saharo-Sindian taxa account for 52.63% of the total number of species documented, and these taxa are either pluri-, bi-, or mono-regional. The ability of Saharo-Sindian and Mediterranean components to penetrate this region might explain the large percentages of this element in the research area, as well as the human effect. In addition, the plant species from the Saharo-Arabian region are species which are strongly adapted to desert conditions, whereas Mediterranean species indicate a more mesic environment [56,57].

3.3. Classification of Vegetation

TWINSPAN categorization was used to identify four vegetation groups based on the importance values of 57 plant species reported in 37 sampled stands in the study area (Figure 2 and Table 2). The detailed importance values of all recorded species were provided in Supplementary Materials Table S4. It should be noted that certain plant categories are representative of one or more of the sites surveyed. Groups I and III were distributed in the sand formation (sand flat) habitat, group II was distributed in sand formation and salt marsh habitats, whereas group IV was restricted to the salt marsh habitat (Table 2).

The community I consists of four stands dominated by *E. spinosus* (IV = 25.53), while the other important species (i.e., attaining relatively high importance values) in this group are *Brassica tournefortii* (IV = 20.29), *Bromus diandrus* (IV = 18.38), *Acacia saligna* (IV = 17.19) and *Mesembryanthemum crystallinum* (IV = 17.23). The indicator species in this group are *B. tournefortii* (IV = 20.29) and *Zygophyllum aegyptium* (IV = 1.86). The sites were characterized by high percentages of soil fraction (silt and clay), pH, Cl^- , SO_4^{2-} , SAR, and moderate contents of organic carbon (Table 3).

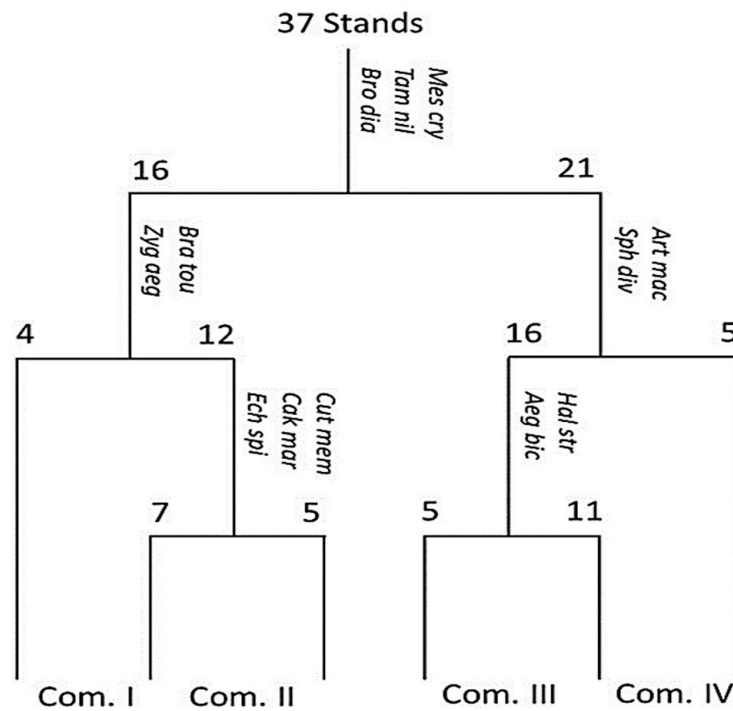


Figure 2. TWINSpan dendrogram of 37 stands based on the important value of plant species. The first three letters of both the genus and species names are an abbreviation of the indicator species names. *Mes cry*: *Mesembryanthemum crystallinum*, *Tam nil*: *Tamarix nilotica*, *Bro dia*: *Bromus diandrus*, *Art mac*: *Arthrocnemum macrostachyum*, *Sph div*: *Sphenopus divaricatus*, *Bra tou*: *Brassica tournefortii*, *Zyg aeg*: *Zygophyllum aegyptium*, *Hal str*: *Halocnemum strobilaceum*, *Aeg bic*: *Aegilops bicornis*, *Cut mem*: *Cutandia memphitica*, *Cak mar*: *Cakile maritima*, *Ech spi*: *Echinopus spinosus*.

Table 2. Characteristics of the different communities (I–IV) from TWINSpan classification of the studied area.

Com.	Stand No.	Total Species	Habitats	Dominant Species (IV ± SD)	Other Important Species
I	4	25	SF	<i>Echinopus spinosus</i> (25.53 ± 0.79) *	<i>Brassica tournefortii</i> (20.29 ± 0.70) <i>Bromus diandrus</i> (18.38 ± 0.79) <i>Acacia saligna</i> (17.19 ± 2.00) <i>Mesembryanthemum crystallinum</i> (17.23 ± 1.52) <i>Rumex pictus</i> (13.26 ± 1.27) <i>Malva parviflora</i> (10.62 ± 0.83)
II	12	43	SF, SM	<i>Zygophyllum aegyptium</i> (25.42 ± 0.60) <i>Calligonum polygnoides</i> (23.14 ± 2.00)	<i>Senecio glaucus</i> (19.04 ± 0.44) <i>Cakile maritima</i> (13.93 ± 1.01) <i>Bromus diandrus</i> (13.63 ± 0.89) <i>Echinopus spinosus</i> (12.76 ± 0.93) <i>Poa annua</i> (11.37 ± 0.81) <i>Rumex pictus</i> (10.51 ± 0.78)
III	16	41	SF	<i>Calligonum polygnoides</i> (38.20 ± 0.54)	<i>Iflora spicata</i> (18.84 ± 0.63) <i>Senecio glaucus</i> (16.94 ± 0.55) <i>Lotus halophilus</i> (11.96 ± 0.72) <i>Rumex pictus</i> (11.58 ± 0.59) <i>Tamarix nilotica</i> (11.00 ± 0.88) <i>Cutandia memphitica</i> (10.54 ± 1.53)
IV	5	24	SM	<i>Arthrocnemum macrostachyum</i> (32.99 ± 0.49) <i>Sphenopus divaricatus</i> (30.61 ± 0.49)	<i>Iflora spicata</i> (17.08 ± 1.00) <i>Rumex pictus</i> (14.15 ± 0.62) <i>Senecio glaucus</i> (13.59 ± 0.64) <i>Lotus halophilus</i> (11.12 ± 0.92) <i>Tamarix nilotica</i> (11.03 ± 1.40)

* values are average ± SD, SF: sand-flat, SM: salt marshes.

Table 3. Soil physical and chemical analysis of the four identified vegetation groups (I–IV) of the study area.

Sediment Variables	Mean (n = 24)	TWINSPAN Vegetation Groups				LSD _{0.05}
		I (n = 4)	II (n = 12)	III (n = 16)	IV (n = 5)	
Sand (%)	89.76 ± 0.84 #	88.07 ^a ± 1.87	88.37 ^a ± 0.65	90.16 ^a ± 0.30	92.44 ^a ± 0.55	4.99 ^{ns}
Silt (%)	6.79 ± 0.52	7.12 ^a ± 0.91	7.75 ^a ± 0.43	6.98 ^a ± 0.27	5.29 ^b ± 0.45	1.22 ^{**}
Clay (%)	3.46 ± 0.36	4.81 ^a ± 0.97	3.88 ^{ab} ± 0.27	2.86 ^b ± 0.04	2.27 ^b ± 0.15	1.88 ^{ns}
Porosity (%)	38.27 ± 1.16	39.59 ^a ± 2.31	41.95 ^a ± 0.53	32.14 ^b ± 0.43	39.40 ^a ± 1.35	5.84 [*]
WHC (%)	35.98 ± 0.98	32.48 ^b ± 0.99	41.93 ^a ± 1.36	34.10 ^b ± 0.45	35.42 ^b ± 1.11	6.21 [*]
CaCO ₃ (%)	5.65 ± 0.43	5.42 ^a ± 0.61	5.08 ^a ± 0.22	6.42 ^a ± 0.21	5.67 ^a ± 0.68	1.92 ^{ns}
OC (%)	0.40 ± 0.04	0.35 ^a ± 0.07	0.34 ^a ± 0.02	0.34 ^a ± 0.02	0.55 ^a ± 0.06	0.41 ^{ns}
pH	8.36 ± 0.13	9.36 ^a ± 0.13	8.07 ^a ± 0.07	7.55 ^a ± 0.12	8.46 ^a ± 0.18	2.26 ^{ns}
EC (mS.cm ⁻¹)	0.95 ± 0.04	0.74 ^a ± 0.07	0.99 ^a ± 0.05	0.62 ^a ± 0.01	1.44 ^a ± 0.04	5.72 ^{ns}
Cl ⁻ (%)	0.53 ± 0.15	0.83 ^a ± 0.29	0.59 ^b ± 0.07	0.14 ^c ± 0.01	0.57 ^b ± 0.23	0.19 ^{***}
SO ₄ ²⁻ (%)	0.52 ± 0.11	0.66 ^a ± 0.21	0.56 ^a ± 0.05	0.32 ^a ± 0.02	0.53 ^a ± 0.16	0.94 ^{ns}
HCO ₃ ⁻ (%)	0.67 ± 0.10	0.21 ^d ± 0.01	0.54 ^c ± 0.08	1.15 ^a ± 0.09	0.77 ^b ± 0.21	0.06 ^{***}
Na ⁺ (mg/100 g dry soil)	137.64 ± 12.52	91.75 ^c ± 3.62	150.32 ^b ± 12.74	237.75 ^a ± 18.75	70.75 ^d ± 14.97	10.17 ^{***}
K ⁺ (mg/100 g dry soil)	45.42 ± 4.63	15.05 ^c ± 0.52	54.06 ^b ± 6.75	100.32 ^a ± 8.80	12.24 ^c ± 2.45	3.58 ^{***}
Ca ⁺⁺ (mg/100 g dry soil)	41.63 ± 3.74	23.21 ^c ± 1.00	47.83 ^b ± 4.75	81.08 ^a ± 6.55	14.40 ^d ± 2.64	7.15 ^{***}
Mg ⁺⁺ (mg/100 g dry soil)	52.01 ± 5.40	11.63 ^c ± 0.28	57.27 ^b ± 7.61	126.66 ^a ± 11.35	12.46 ^c ± 2.37	4.52 ^{***}
SAR	19.27 ± 1.16	21.92 ^a ± 0.49	19.62 ^{ab} ± 0.71	19.69 ^{ab} ± 0.72	15.86 ^b ± 2.70	5.84 ^{ns}
PAR	4.50 ± 0.32	3.60 ^{bc} ± 0.06	4.97 ^{ab} ± 0.36	6.64 ^a ± 0.37	2.77 ^c ± 0.50	2.17 [*]

Mean values ± standard error, WHC: Water-holding capacity, OC: organic carbon, EC: electric conductivity, SAR: sodium adsorption ratio, PAR: potassium adsorption ratio, superscript letter within each row shows significant variation at $p < 0.05$. ns: non-significant, * $p < 0.05$, ** $p < 0.01$, *** $p < 0.001$.

Community II includes 12 stands, co-dominated by *Z. aegyptium* (IV = 25.42) and *C. polygoides* (IV = 23.14). The other important species in this group are *S. glaucus* (IV = 19.04), *Cakile maritima* (IV = 13.93), and *B. diandrus* (IV = 13.63). In this group, the indicator species are *C. memphitica* (IV = 7.72), *C. maritima* (IV = 13.93), and *E. spinosus* (IV = 12.76). This group's stands were discovered on soil with high fine sand and clay content, porosity and WHC, and intermediate electrical conductivity, cations, and anions (Table 3).

Community III consists of 16 stands dominated by *C. polygoides* (IV = 38.20). In this group, the other important species are *I. spicata* (IV = 18.84), *S. glaucus* (IV = 16.94), and *L. halophilus* (IV = 11.96). The indicator species are *Halocnemum strobilaceum* (IV = 7.21) and *Aegilops bicornis* (IV = 10.34). Most of the examined soil variables (sand, Na⁺, K⁺, Ca²⁺, Mg²⁺, HCO₃⁻, CaCO₃) attained their highest levels in the stands of this group (Table 3). Community IV consist of five stands co-dominated by halophytes; *Arthrocnemum macrostachyum* (IV = 32.99) and *Sphenopus divaricatus* (IV = 30.61). The other important species are *I. spicata* (IV = 17.08) and *R. pictus* (IV = 14.15). The indicator species in this group include *A. macrostachyum* (IV = 32.99) and *S. divaricatus* (IV = 30.61). The stands were found to have the highest levels of fine sand, electric conductivity, organic carbon, pH, as well as moderate contents of HCO₃⁻, CaCO₃ (Table 3). El-Amier, et al. [49] reported that *E. spinosus* and *C. polygoides* are found in the sand flats and mounds along the Mediterranean coast associated with *B. tournefortii*, *B. diandrus*, *M. crystallinum*, *S. glaucus*, *C. maritima*, *I. spicata*, and *R. pictus*. In the salt marshes of the Mediterranean coast, Zahran and El-Amier [58] found that *A. macrostachyum*, *S. divaricatus*, and *Z. aegyptium* are prevalent, along with *I. spicata*, *S. glaucus*, *H. strobilaceum*, *Tamarix nilotica*, *Spergularia marina*, *S. divaricatus*, and *Stipagrostis lanata*. This group is consistent with studies indicating that the vegetation of Mediterranean coastal strip is dominated by many herbs, shrubs, and some trees, and therefore has high species richness and plant cover [48,49,56,59].

3.4. Ordination of Sampling Sites

The ordination of sampled stands given by DCA is shown in Figure 3. The TWINSPAN vegetation groups were clearly distinguishable and had a comprehensible pattern of segregation on the ordination plane, with groups I and II separated at the upper part of the left zone of the DCA diagram, and group III separated at the middle part of the right zone, as well as a superimposed intercept with group II. Group IV is clearly separated in the

lower part of the left zone of the DCA diagram. Along the DCA ordination axes, these groups were clearly differentiated. It's worth noting that the strong parallels in floristic composition and natural habitats between the above-mentioned plant types may explain interspecific interactions [49,56].

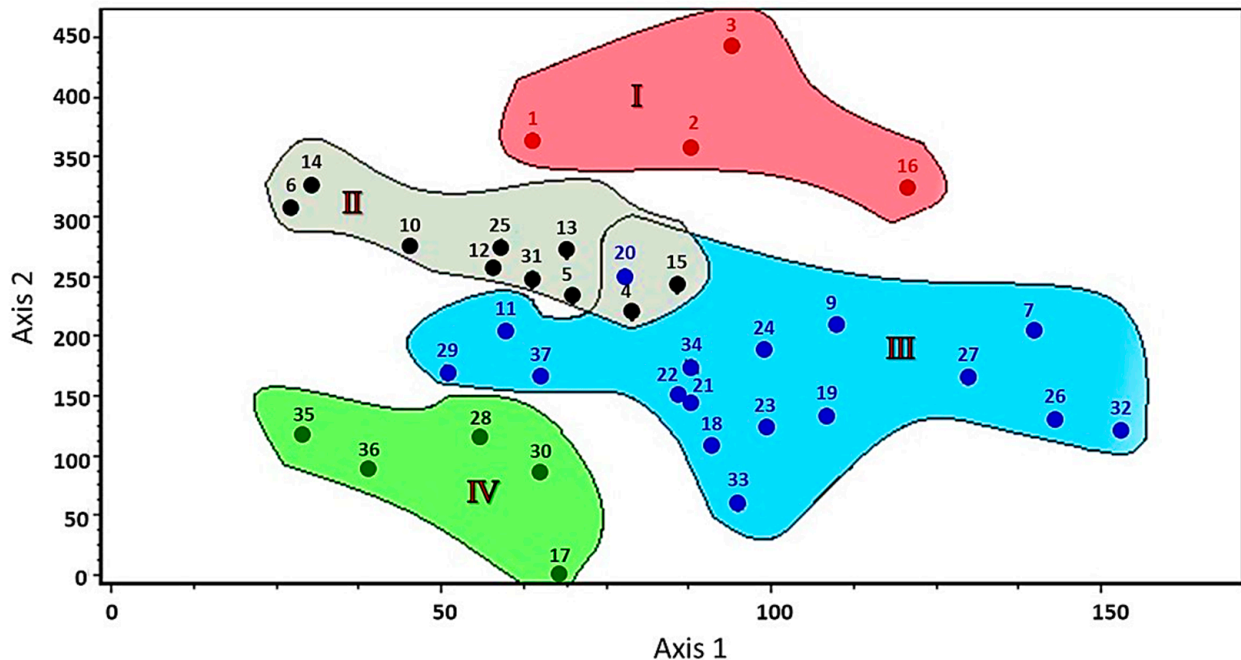


Figure 3. Detrended Correspondence Analysis (DCA) ordination diagram of the 37 stands with vegetation groups of the Deltaic Mediterranean coastal area (Dakahlia Governorate). The stands were numbered from 1 to 37 and represented by “•”.

3.5. Soil–Vegetation Relationships

The plant species diversity of natural communities can be influenced by soil texture, salinity, organic carbon, and nutrient availability [56,60]. The ordination diagram of the species–environment biplot obtained by Canonical Correspondence Analysis (CCA) depicts the relationship between the detected plant categories and soil properties. As indicated in Figure 4, the most important soil variables with strong significant correlations with the first and second axes are electrical conductivity, cations, organic carbon, porosity, potassium adsorption ratio (PAR), chlorides, and bicarbonates.

In the upper right side of the CCA diagram, *Calligonum polygnaoides* (co-dominant species in community II and dominant in community III) showed a close correlation to soil cations (calcium, potassium, magnesium, and sodium), potassium adsorption ratio, and sand. On the other hand, the *Arthrocnemum macrostachyum* (dominant species of community IV), *S. divaricatus* (dominant species of community IV), and *Senecio glaucus* were plotted in the lower-right side of the CCA diagram, where they showed a correlation to organic matter content. On the same side, the *Lotus spicatus*, *Lotus halophilus*, and *Tamarix nilotica* showed a close correlation to bicarbonates and calcium carbonate content (Figure 4).

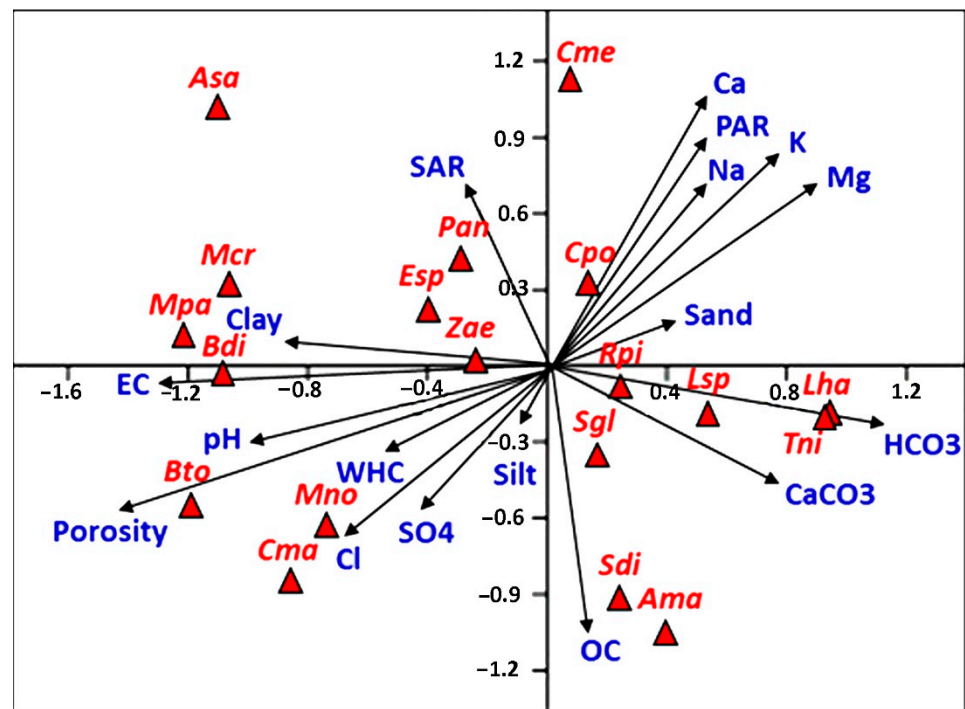


Figure 4. Canonical Correspondence Analysis (CCA) biplot of species–soil variable. EC: electrical conductivity, OC: organic carbon, SAR: sodium adsorption ratio, PAR: potassium adsorption ratio, WHC: water-holding capacity, Cme: *Cutandia memphitica*, Cpo: *Calligonum polygoides*, Rpi: *Rumex pictus*, Lsp: *Lotus spicatus*, Lha: *Lotus halophilus*, Tni: *Tamarix nilotica*, Sgl: *Senecio glaucus*, Sdi: *Sphenopus divaricatus*, Ama: *Arthrocnemum macrostachyum*, Mno: *Mesembryanthemum nodiflorum*, Cma: *Cakile maritima*, Bto: *Brassica tournefortii*, Zae: *Zygophyllum aegyptium*, Esp: *Echinopus spinosus*, Pan: *Poa annua*, Bdi: *Bromus diandrus*, Mpa: *Malva parviflora*, Mcr: *Mesembryanthemum crystallinum*, Asa: *Acacia saligna*.

On the upper-left side of the CCA biplot, *Mesembryanthemum crystallinum*, *Malva parviflora*, *Zygophyllum aegyptium* (dominant in community II), and *Echinopus spinosus* (dominant in community I) showed a correlation to salinity and clay content. Meanwhile, on the lower-left side, *Brassica tournefortii*, *Mesembryanthemum nodiflorum*, and *Cakile maritima* were closely correlated to the water-holding capacity, pH, porosity, chloride, and sulfate.

The results of the CCA for soil variables are presented in Supplementary Materials Table S5. The three main axes of CCA explained 68.81% of the total variance based on eigenvalues (eigenvalue < 1) (Supplementary Materials Table S5). The first CCA (axis 1) explains 13.16% of the total variance and consists of EC, HCO₃, cations, and PAR. These metals are associated with the first component matrix (PC1), which shows high values in the first component. This finding might mean that electrical conductivity is directly proportional to cations and anions. The second CCA (Axis 2) explains 11.12% of the total variance and consists of cations, SAR, and PAR. The fact that these variables have higher loading factors in the first component suggests that the same sources, such as wastewater, industrial pollution, and anthropogenic activities, may be controlling the salinity.

3.6. Spectral Analysis

3.6.1. LULC analysis

The analysis of remotely sensed data to detect the changes in the LULC explains the impact of different anthropogenic activities such as industrialization, modernization, reclamation, urbanization, and other practices on the environmental resources. The total areas and the annual rates of increase/decrease for each class are illustrated in Figure 5.

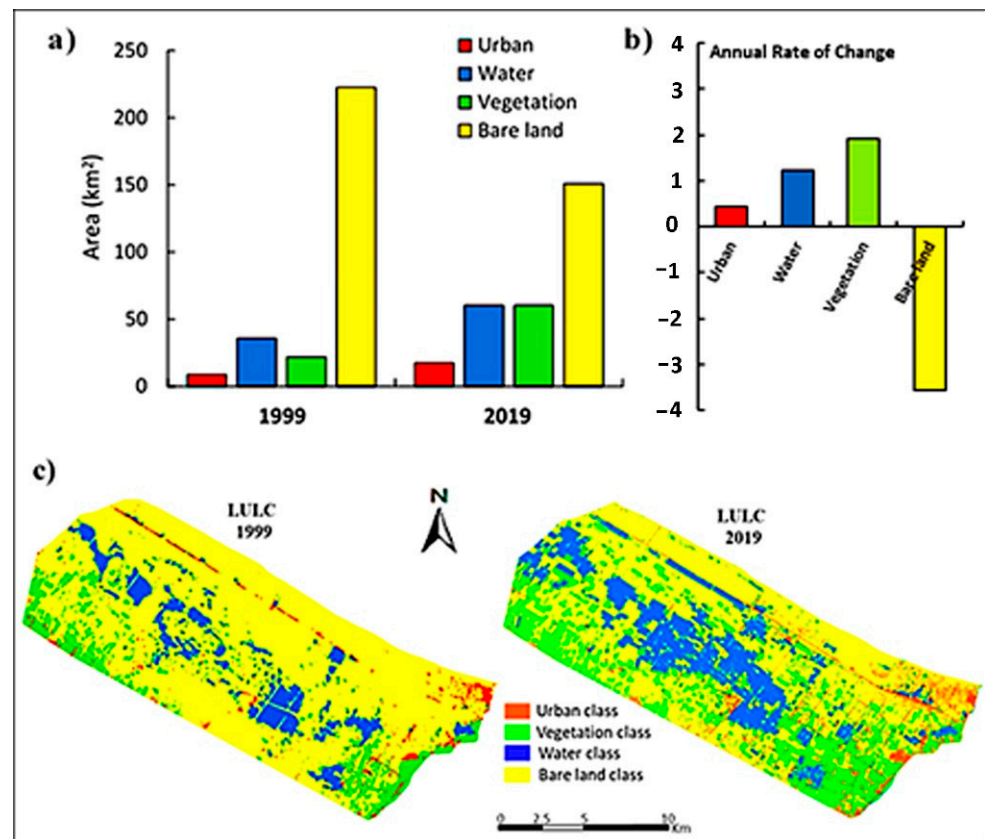


Figure 5. Areas in sq. km of LULC classification for Deltaic Mediterranean Coast of the study area (a) classification comparison from 1999 to 2019, (b) annual rate of change for each class, and (c) LULC distribution map.

It was found that the coastal region was subject to dramatic spatial and temporal changes during the investigated period. A clear decrease in the most dominant class was observed: Bare land class decreased from 222.47 km² (77.02%) in 1999 to 151.18 km² (52.34%) in 2019. The second most dominant class was water bodies, occupying an area of 35.85 km² (12.41%) and 60.24 km² (20.86%) in the years 1999 and 2019, respectively. In addition, the vegetation class increased by 21.86 km² (7.57%) in 1999 to 60.11 km² (20.81%) in 2019. The urban class took the last position; however, it presented an increase of 8.65 km² (3.00%) to 17.29 km² (5.99%) between the years 1999 and 2019, as shown in Figure 5. From the analysis of the LULC data, it is clear that the huge decrease in the bare land class was in favor of the increase in the vegetation, water, and urban classes, taking into account that the increase in water class could be due to the expansion of pisciculture (fish culture) as well as the wetlands caused by seawater leaching [61]. Moreover, the scattering of the agricultural lands, thereby explaining the increase in the vegetation class including wild habitats spreading due to the existence of favorable conditions [62,63], to meet the resident needs, will positively affect the water represented in the water canals needed for this scattering.

Accordingly, investment in the construction of new residential areas, e.g., new Mansoura, may explain the increase in the urban class. Furthermore, in order to meet the needs of this urban crawling, bare land surrounding the new residential areas is being converted into agricultural land. In other words, along with the construction of new residential areas, there will be an increase in agriculture and water supplies to meet resident needs, which explains the increase in the urban, vegetation, and water class at the expense of the bare land class [64].

3.6.2. Spectral Indices Assessment Change Detection in NDVI

Vegetation indices (VI), the most common of which is NDVI, are metrics that employ spectral reflectance relevant to plants. NDVI is a common approach for assessing the productivity of vegetation, or “greenness”, in a specified region, since it is sensitive to active photosynthetic compounds [17,65]. Regarding the coastal study area, the wild plant habitats were most accurately represented by the sparse vegetation class when compared to the other vegetation classes. The application of the NDVI was necessary to differentiate the vegetation classes and to detect the change over the last two decades in the wild plant habitats that are included in the sparse vegetation, which showed the highest increase from 21.23 km² in 1999 to 77.44 km² in 2019 with an annual increase detected of 2.81 km². On the other hand, the dense vegetation class slightly increased from 0.46 km² in 1999 to 2.97 km² in 2019. Likewise, moderate vegetation occupied 10.27 km² in 1999 and 41.77 km² in 2019. Finally, no vegetation class showed a noticeable decrease from 254.83 km² in 1999 to 164.64 km² in 2019, which occurred as a result of the increase in the other three classes (Figure 6).

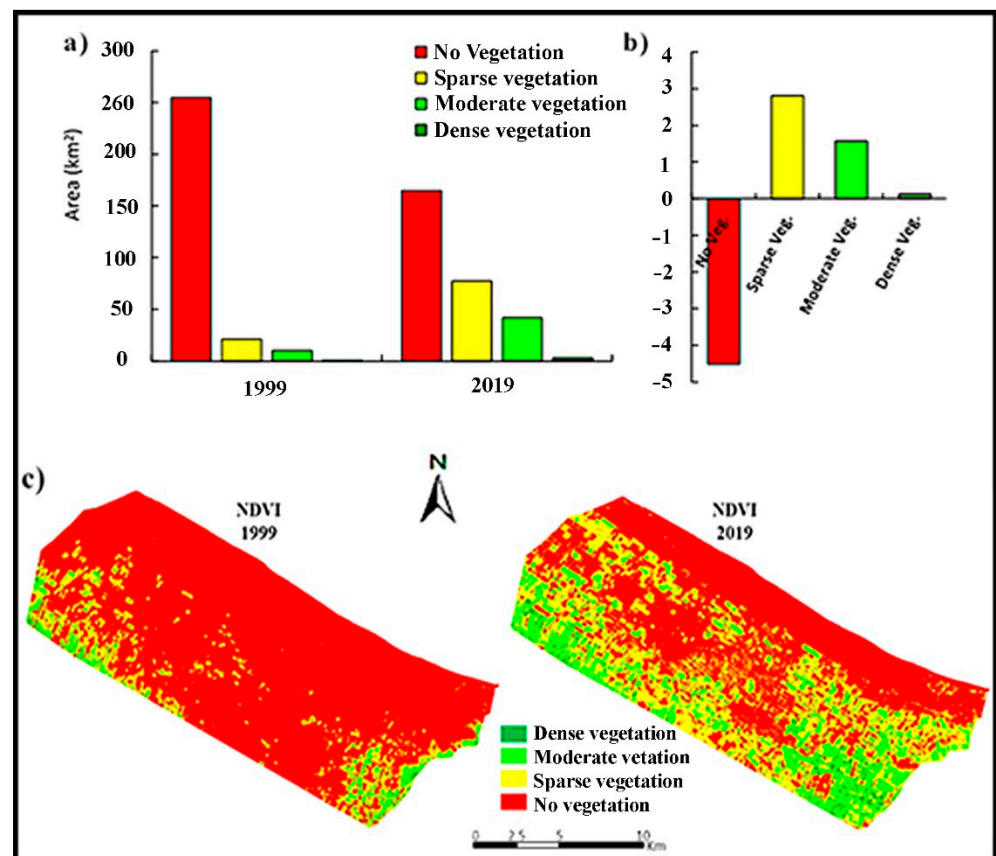


Figure 6. Areas in sq. km of NDVI classification for Deltaic Mediterranean Coast of the study area; (a) classification comparison from 1999 to 2019, (b) annual rate of change for each class, and (c) NDVI distribution map.

Moreover, this spread may be threatened in the future by urban crawling, which consequently changes the soil character, turning the habitat unfavorable for the flourishing of wild plants. Human activity endangers biodiversity in at least five main ways. The first, agricultural and industrial expansion, has led to the loss of over 85% of wetlands, altered 75% of the land surface, and impacted 66% of the ocean area, as described in IPCC [66]. A second powerful threat is the exploitation of plant species through overharvesting and logging. Third is pollution: habitats are being destroyed by untreated waste; by pollutants

from industrial, mining, and agricultural activities; and by oil spills and toxic dumping. A fourth critical driver of biodiversity loss is the introduction of non-indigenous species that edge out native ones; this has increased by 40% globally over the same period. Fifth, climate change exacerbates nature's loss, which in turn reduces nature's resilience to climate change [66]. The moderate and dense vegetation class represented an increase in agricultural lands that accompanied urban crawling and residential services. Accordingly, this increase in the sparse, moderate, and dense vegetation classes is compensated by a decrease in the no vegetation class [67].

Change Detection in NDMI and NDSI

NDMI is used to monitor changes in the water content of leaves and was proposed by Gao [68]. The interpretation of the absolute value of the NDMI makes it possible to immediately recognize the areas of the farm or field with water stress problems. According to the data analysis, the NDMI fluctuated between -0.35 and 0.89 in 1999, with a mean value of 0.03 . However, it later climbed in 2019 from -0.86 to 0.66 , with a mean value of 0.15 . (Figure 7). These findings are significantly connected to the rise in NDVI (sparse vegetation), which was previously described in the LULC assessment, and NDVI that corresponds with the LULC analysis [69]. Moisture elevation might be explained by an increase in moisture levels caused by the quantitative rise of wild plant species and their flourishing as a result of the low water stress in the study area, causing the MI mean value to clearly increase, as indicated by [68].

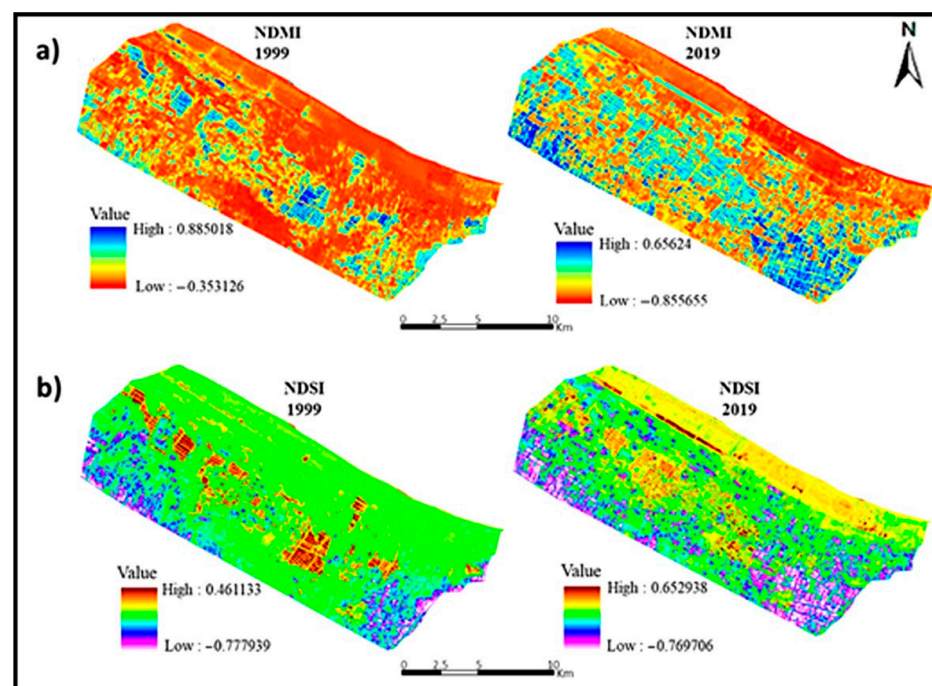


Figure 7. (a) Spatial distribution maps of NDMI, (b) spatial distribution maps of NDSI; for Deltaic Mediterranean Coast of the study area.

Soil salinization is a process of enriching the soil with soluble salts to deleterious levels at or near the soil surface, resulting in modification of biochemical features of soil [70]. Saline intrusion occurs when salts are dissolved in water to accumulate in the soil at a level that affects agricultural production, environment, and economics. NDSI has been proven to have high potential in the enhancement and extraction of soil salinity from remote sensing data [71]. In the present investigation, NDSI ranged from -0.78 to 0.46 with a mean of -0.10 in 1999, and decreased to a range from -0.77 to 0.65 with a mean of -0.27 in 2019 (Figure 8). The obvious decrease in the salinity index might be attributed to the previously reported increase in water levels in the LULC assessment, as shown in

Figure 7, which produced dilution of the soil salinity levels. Furthermore, this drop favored the flourishing and growth in the NDVI (sparse vegetation) that represents wild habitats. This demonstrates the negative association between the NDSI and the NDVI in the current research region. Moreover, this could be an indicator of the reason why most of the wild plants presented in the wild habitats in the coastal region of Dakahlia Governorate are not adaptive to high salinity [72].

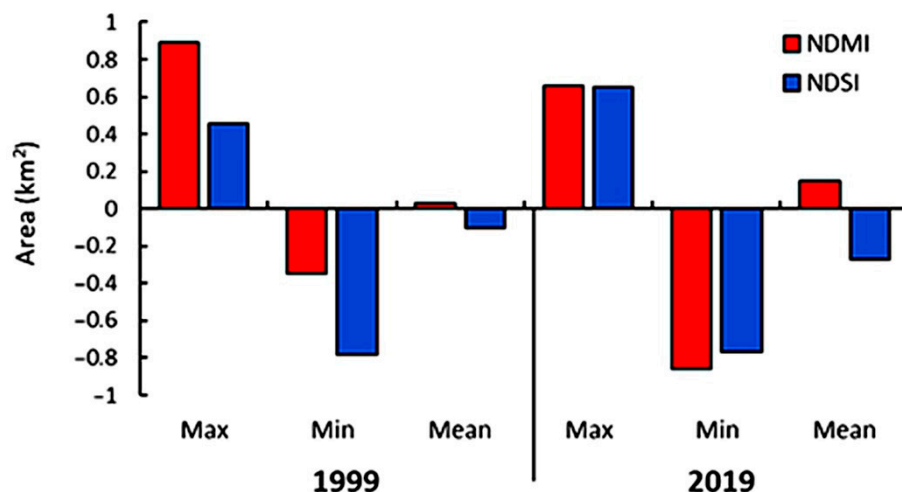


Figure 8. Statistics of the spectral retrieved parameters for Deltaic Mediterranean Coast of the study area.

4. Conclusions

The Nile Delta Mediterranean coast of the Dakahlia Governorate indicated the presence of several communities, the majority of which were dominated by halophytes and sand dune plants. The plants primarily inhabiting the sand flats and salt marshes habitats flourished with increased soil fertility and oxygen levels. The strong, directly proportional relationship between an increase in NDVI and an increase in NDMI along the deltaic Mediterranean coast—which was not conditionally dependent on soil salinity levels (NDSI) but was primarily dependent on the detected species in the study area and which aided in their flourishing—was supported by this. Following the evaluation of the preceding indices, the NDVI indicated a significant increase in the total consumed surface by the sparse vegetation class from 21.24 in 1999 to 77.45 in 2019. Similarly, the mean moisture index increased from 0.03 to 0.15, while the salinity index decreased from -0.10 to -0.27 . Finally, the development of waterlogging and fish farming resulted in a decrease in soil salinity throughout the deltaic Mediterranean shores, which promoted the ideal circumstances for the spread of wild plant habitats. It may be stated that remote sensing and geographic information systems (GIS) are becoming more popular technologies for evaluating and managing large volumes of regional data. In landscape design and area management planning, tracking changes in usage and showing the findings is critical.

Supplementary Materials: The following are available online at <https://www.mdpi.com/article/10.3390/agriculture12010108/s1>, Table S1: Coordinates and description of sampling sites along the Nile Delta Mediterranean coast of the Dakahlia Governorate, Table S2: The enumerated list of plant species along the Nile Delta Mediterranean coast of the Dakahlia Governorate, together with their families, growth forms, chorotypes, and presence percentage, Table S3: The number of species and percentage of various floristic categories of the Nile Delta Mediterranean coast of the Dakahlia Governorate, Table S4: The abundance of various plant species within the four identified vegetation groups along the Nile Delta coast of the Dakahlia Governorate, Table S5: CCA biplot scores for soil variables from different sites of the studied area

Author Contributions: Conceptualization, A.E.-Z., S.A.E., H.N.-E., A.M.A.-E. and Y.A.E.-A.; formal analysis, A.E.-Z., S.A.E., H.N.-E., A.M.A.-E. and Y.A.E.-A.; investigation, A.E.-Z., S.A.E., H.N.-E., E.-S.F.E.-H., G.B., A.M.A.-E. and Y.A.E.-A.; validation, A.E.-Z., S.A.E., H.N.-E., A.M.A.-E. and Y.A.E.-A.; writing—original draft preparation, A.E.-Z., S.A.E., H.N.-E., A.M.A.-E. and Y.A.E.-A.; writing—review and editing, A.E.-Z., S.A.E., H.N.-E., A.M.A.-E., G.B., W.S. and Y.A.E.-A. All authors have read and agreed to the published version of the manuscript.

Funding: This research was funded by the Researchers Supporting Project number (RSP-2021/390), King Saud University, Riyadh, Saudi Arabia.

Institutional Review Board Statement: Not Applicable.

Informed Consent Statement: Not Applicable.

Data Availability Statement: Not Applicable.

Acknowledgments: The authors want to thank the Researchers Supporting Project number (RSP-2021/390), King Saud University, Riyadh, Saudi Arabia.

Conflicts of Interest: The authors declare no conflict of interest.

References

1. Venâncio, C.; Ribeiro, R.; Lopes, I. Seawater intrusion: An appraisal of taxa at most risk and safe salinity levels. *Biol. Rev.* **2021**, *97*, 361–382. [[CrossRef](#)]
2. Jiang, L.; Bao, A.; Guo, H.; Ndayisaba, F. Vegetation dynamics and responses to climate change and human activities in Central Asia. *Sci. Total Environ.* **2017**, *599*, 967–980. [[CrossRef](#)]
3. Postel, S.; Richter, B. *Rivers for Life: Managing Water for People and Nature*; Island Press: Washington, DC, USA, 2012.
4. Zahran, M.A.; Willis, A.J. *The Vegetation of Egypt*; Springer Science & Business Media: Berlin/Heidelberg, Germany, 2009; Volume 2.
5. Balmford, A.; Bruner, A.; Cooper, P.; Costanza, R.; Farber, S.; Green, R.E.; Jenkins, M.; Jefferiss, P.; Jessamy, V.; Madden, J.; et al. Economic reasons for conserving wild nature. *Science* **2002**, *297*, 950–953. [[CrossRef](#)]
6. Costanza, R.; Daly, H.; Goodland, R.; Norgaard, R.B. *An Introduction to Ecological Economics*; CRC Press: Boca Raton, FL, USA, 1997.
7. Zlinszky, A.; Heilmeyer, H.; Balzter, H.; Czúcz, B.; Pfeifer, N. Remote Sensing and GIS for Habitat Quality Monitoring: New Approaches and Future Research. *Remote Sens. Environ.* **2015**, *7*, 7987–7994. [[CrossRef](#)]
8. Seress, G.; Lipovits, Á.; Bókony, V.; Czúni, L. Quantifying the urban gradient: A practical method for broad measurements. *Landsc. Urban Plan.* **2014**, *131*, 42–50. [[CrossRef](#)]
9. Xu, L.; Ivanov, P.C.; Hu, K.; Chen, Z.; Carbone, A.; Stanley, H.E. Quantifying signals with power-law correlations: A comparative study of detrended fluctuation analysis and detrended moving average techniques. *Phys. Rev.* **2005**, *71*, 051101. [[CrossRef](#)]
10. Elagami, S.A.; El-Zeiny, A.; El-Halawany, E.S.F.; El-Amier, Y.A. Monitoring Spatiotemporal Environmental Changes in Dakahlia Governorate, Egypt Using Landsat Imagery. *Let. Appl. NanoBioSci.* **2022**, *11*, 3843–3853.
11. El-Amier, Y.A.; El-Zeiny, A.; El-Halawany, E.S.F.; Elsayed, A.; El-Esawi, M.A.; Noureldeen, A.; Elagami, S.A. Environmental and Stress Analysis of Wild Plant Habitat in River Nile Region of Dakahlia Governorate on Basis of Geospatial Techniques. *Sustainability* **2021**, *13*, 6377. [[CrossRef](#)]
12. Olorunfemi, I.E.; Fasinmirin, J.T.; Olufayo, A.A.; Komolafe, A.A. GIS and remote sensing-based analysis of the impacts of land use/land cover change (LULCC) on the environmental sustainability of Ekiti State, southwestern Nigeria. *Environ. Dev. Sustain.* **2020**, *22*, 661–692. [[CrossRef](#)]
13. Benzer, N. Using the geographical information system and remote sensing techniques for soil erosion assessment. *Pol. J. Environ. Stud.* **2010**, *19*, 881–886.
14. Bing, P.; Hui-min, X.; Tao, H.; Asundi, A. Measurement of coefficient of thermal expansion of films using digital image correlation method. *Polym. Test.* **2009**, *28*, 75–83. [[CrossRef](#)]
15. Bakr, N.; Weindorf, D.C.; Bahnassy, M.H.; Marei, S.M.; El-Badawi, M.M. Monitoring land cover changes in a newly reclaimed area of Egypt using multi-temporal Landsat data. *Appl. Geogr.* **2010**, *30*, 592–605. [[CrossRef](#)]
16. Ormsby, J.P.; Choudhury, B.J.; Owe, M. Vegetation spatial variability and its effect on vegetation indices. *Int. J. Remote Sens.* **1987**, *8*, 1301–1306. [[CrossRef](#)]
17. Tucker, C.J. Red and photographic infrared linear combinations for monitoring vegetation. *Remote Sens. Environ.* **1979**, *8*, 127–150. [[CrossRef](#)]
18. Wiegand, C.L.; Richardson, A.J.; Kanemasu, E.T. Leaf Area Index Estimates for Wheat from LANDSAT and Their Implications for Evapotranspiration and Crop Modeling 1. *Agron. J.* **1979**, *71*, 336–342. [[CrossRef](#)]
19. Chappelle, E.W.; Kim, M.S.; McMurtrey, J.E., III. Ratio analysis of reflectance spectra (RARS): An algorithm for the remote estimation of the concentrations of chlorophyll a, chlorophyll b, and carotenoids in soybean leaves. *Remote Sens. Environ.* **1992**, *39*, 239–247. [[CrossRef](#)]

20. Wiegand, C.L.; Maas, S.J.; Aase, J.K.; Hatfield, J.L.; Pinter, P.J., Jr.; Jackson, R.D.; Lapitan, R.L. Multi-site analyses of spectral-biophysical data for wheat. *Remote Sens. Environ.* **1992**, *42*, 1–21. [[CrossRef](#)]
21. Zahran, M.A.; Willis, A.J. *Plant Life in the River Nile in Egypt*; Mars Publishing House: Reyadh, Saudi Arabia, 2003.
22. UNESCO United Nations Educational. *Map of the World Distribution of Arid Regions*, 7th ed.; MAB Technical Notes; UNESCO: Paris, France, 1979.
23. Ayyad, M.G.; Floc'h, L. *An Ecological Assessment of Renewable Resources for Rural Agricultural Development in the Western Mediterranean Coastal Region of Egypt Case Study: El Omayed Test-Area*; Ministère des Affaires Étrangères and C.N.R.S./C.E.P.E.L. Emberger: Montpellier, France, 1983; 127p.
24. Omran, E.-S.E.; Negm, A.M. Adaptive management zones of Egyptian coastal lakes. In *Egyptian Coastal Lakes and Wetlands: Part I*; Springer: Berlin/Heidelberg, Germany, 2018; pp. 37–60.
25. Shukla, R.S.; Chandel, P.S. *A Textbook of Plant Ecology including Ethobotany and Soil Science*, 10th ed.; S. Chand & Company Ltd.: New Delhi, India, 1989.
26. Canfield, R.H. Application of the line interception method in sampling range vegetation. *J. For.* **1941**, *39*, 388–394.
27. Boulos, L. *Flora of Egypt*; Al Hadara Publishing: Cairo, Egypt, 1999; Volume 1.
28. Boulos, L. *Flora of Egypt*; Al Hadara Publishing: Cairo, Egypt, 2002; Volume 3.
29. Boulos, L. *Flora of Egypt*; Al Hadara Publishing: Cairo, Egypt, 2005; Volume 4.
30. Täckholm, V. *Student's Flora of Egypt*, 2nd ed.; Cairo University Press: Cairo, Egypt, 1974.
31. Raunkjær, C. *Plant Life Forms*; Clarendon Press: Oxford, UK, 1937.
32. Piper, C.S. *Soil and Plant Analysis*; Interscience Publishers, Inc.: New York, NY, USA, 1947.
33. Jackson, M.L. *Soil Chemical Analysis*; Constable and Co., Ltd.: London, UK, 1962.
34. Pierce, W.C.; Haenisch, E.L.; Sawyer, D.T. *Quantitative Analysis*; Wiley Toppen: Tokyo, Japan, 1958.
35. McKell, C.M.; Goodin, J.K. A brief overview of the saline lands of the United States. In *Research and Development Seminar on Forage and Fuel Production from Salt-Affected Wasteland*; CABI: Cunderdin, Australia, 1984.
36. Jensen, J.R. *Introductory Digital Image Processing: A Remote Sensing Perspective*, 2nd ed.; Prentice-Hall Inc.: Hoboken, NJ, USA, 1996.
37. Gad, A.A.; El-Zeiny, A. Spatial analysis for sustainable development of El Fayoum and Wadi El Natrun desert depressions, Egypt with the aid of remote sensing and GIS. *J. Geog. Environ. Earth Sci. Int.* **2016**, *8*, 1–18. [[CrossRef](#)]
38. Rouse, J.W. *Monitoring the Vernal Advancement and Retro Gradation of Natural Vegetation*; NASA: Texas A&M University, Remote Sensing Center: College Station, TX, USA, 1973.
39. Khan, N.M.; Rastoskuev, V.V.; Sato, Y.; Shiozawa, S. Assessment of hydrosaline land degradation by using a simple approach of remote sensing indicators. *Agric. Water Manag.* **2005**, *77*, 96–109. [[CrossRef](#)]
40. Foody, G.; Boyd, D. Detection of partial land cover change associated with the migration of inter-class transitional zones. *Int. J. Remote Sens.* **1999**, *20*, 2723–2740. [[CrossRef](#)]
41. Hill, M.O.; Šmilauer, P. *WinTWINS. TWINSpan for Windows Version, 2.3*; Centre for Ecology and Hydrology, University of South Bohemia: Huntingdon, UK; České Budějovice, Czech, 2005.
42. Ter Braak, C.J. *CANOCO-aFORTRAN Program for Canonical Community Ordination by Partial Detrended Correspondence Analysis, Principal Component Analysis and Redundancy Analysis*; Servier: Amsterdam, The Netherlands, 1988.
43. Van Oudtshoorn, K.v.R.; van Rooyen, M.W. Restriction of dispersal due to reduction of dispersal structures. In *Dispersal Biology of Desert Plants*; Springer: Berlin/Heidelberg, Germany, 1999; pp. 93–119.
44. Stanley, K.E. *Evolutionary Trends in the Grasses (Poaceae): A Review*; Michigan Publishing, University of Michigan Library: Ann Arbor, MI, USA, 1999.
45. Funk, V.A.; Susanna, A.; Stuessy, T.; Bayer, R. *Systematics, Evolution, and Biogeography of the Compositae*; IAPT: Vienna, Austria, 2009.
46. Walters, D.R.; Keil, D.J. *Vascular Plant Taxonomy*; Kendall Hunt: Dubuque, IO, USA, 1996.
47. El-Amier, Y.A. Vegetation structure and soil characteristics of five common geophytes in desert of Egypt. *Egypt. J. Basic Appl. Sci.* **2016**, *3*, 172–186. [[CrossRef](#)]
48. Abd-ElGawad, A.M.; El-Amier, Y.A.; Assaeed, A.M.; Al-Rowaily, S.L. Interspecific variations in the habitats of *Reichardia tingitana* (L.) Roth leading to changes in its bioactive constituents and allelopathic activity. *Saudi J. Biol. Sci.* **2020**, *27*, 489–499. [[CrossRef](#)] [[PubMed](#)]
49. El-Amier, Y.A.; El-Halawany, E.F.; Abdullah, T.J. Composition and diversity of plant communities in sand formations along the northern coast of the Nile Delta in Egypt. *Res. J. Pharm. Biol. Chem. Sci.* **2014**, *5*, 826–847.
50. Abd El-Gawad, A.M. Ecology and allelopathic control of *Brassica tournefortii* in reclaimed areas of the Nile Delta, Egypt. *Turk. J. Bot.* **2014**, *38*, 347–357. [[CrossRef](#)]
51. Asri, Y. *Plant Diversity in Touran Biosphere Reservoir*; Publishing Research Institute of Forests and Rangelands: Tehran, Iran, 2003; p. 306.
52. El-Husseini, N.; El-Ghani, M.M.A.; El-Naggar, S.M. Biogeography and diversity of the tubiflorae in Egypt. *Pol. Bot. J.* **2008**, *53*, 105–124.
53. Danin, A.; Orshan, G. The distribution of Raunkiaer life forms in Israel in relation to the environment. *J. Veg. Sci.* **1990**, *1*, 41–48. [[CrossRef](#)]

54. El-Amier, Y.A.; Abdul-Kader, O.M. Vegetation and species diversity in the northern sector of Eastern Desert, Egypt. *West Afr. J. Appl. Ecol.* **2015**, *23*, 75–95.
55. El Hadidi, M.N. Natural vegetation. In *The Agriculture in Egypt*; Oxford University Press: Oxford, UK, 1993; Volume 3.
56. El-Amier, Y.A.; El Hayyany, L.Y. Floristic composition and species diversity of plant communities associated with genus *Atriplex* in Nile Delta coast, Egypt. *Asian J. Conserv. Biol.* **2020**, *9*, 11–24.
57. El-Demerdash, M.; Hegazy, A.; Zilay, A. Distribution of the plant communities in Tihamah coastal plains of Jazan region, Saudi Arabia. *Vegetation* **1994**, *112*, 141–151. [[CrossRef](#)]
58. Zahran, M.A.; El-Amier, Y.A. Non-traditional fodders from the halophytic vegetation of the deltaic Mediterranean coastal desert Egypt. *J. Biol. Sci.* **2013**, *13*, 226–233. [[CrossRef](#)]
59. Al-Rowaily, S.L.; Abd-ElGawad, A.M.; Alghanem, S.M.; Al-Taisan, W.a.A.; El-Amier, Y.A. Nutritional Value, Mineral Composition, Secondary Metabolites, and Antioxidant Activity of Some Wild Geophyte Sedges and Grasses. *Plants* **2019**, *8*, 569. [[CrossRef](#)]
60. Andreasen, C.; Skovgaard, I.M. Crop and soil factors of importance for the distribution of plant species on arable fields in Denmark. *Agric. Ecosyst. Environ.* **2009**, *133*, 61–67. [[CrossRef](#)]
61. Allam, M.; Bakr, N.; Elbably, W. Multi-temporal assessment of land use/land cover change in arid region based on landsat satellite imagery: Case study in Fayoum Region, Egypt. *Remote Sens. Appl. Soc. Environ.* **2019**, *14*, 8–19. [[CrossRef](#)]
62. Bossard, C.; Randall, J.; Hoshovsky, M. *Invasive Plants of California's Wildlands*; University of California Press: Berkeley, CA, USA, 2000; p. 360.
63. Vivekananda, G.; Swathi, R.; Sujith, A. Multi-temporal image analysis for LULC classification and change detection. *Eur. J. Remote Sens.* **2021**, *54*, 189–199. [[CrossRef](#)]
64. El-Zeiny, A.M.; Effat, H.A. Environmental analysis of soil characteristics in El-Fayoum Governorate using geomatics approach. *Environ. Monit. Assess.* **2019**, *191*, 463. [[CrossRef](#)] [[PubMed](#)]
65. Tucker, C.J.; Gatlin, J.A.; Schneider, S.R. Monitoring vegetation in the Nile Delta with NOAA-6 and NOAA-7 AVHRR imagery. *Photogramm. Eng. Remote Sens.* **1984**, *50*, 53–61.
66. International Panel on Climate Change. Summary for Policymakers. In *Global Warming of 1.5 °C: An IPCC Special Report*; World Meteorological Organization: Geneva, Switzerland, 2018.
67. Eid, A.N.M.; Olatubara, C.; Ewemoje, T.; Farouk, H.; El-Hennawy, M.T. Coastal wetland vegetation features and digital Change Detection Mapping based on remotely sensed imagery: El-Burullus Lake, Egypt. *Int. Soil Water Conserv. Res.* **2020**, *8*, 66–79.
68. Gao, B.-C. NDWI—A normalized difference water index for remote sensing of vegetation liquid water from space. *Remote Sens. Environ.* **1996**, *58*, 257–266. [[CrossRef](#)]
69. Karan, S.K.; Samadder, S.R.; Maiti, S.K. Assessment of the capability of remote sensing and GIS techniques for monitoring reclamation success in coal mine degraded lands. *J. Environ. Manag.* **2016**, *182*, 272–283. [[CrossRef](#)]
70. Metternicht, G.; Zinck, A. *Remote Sensing of Soil Salinization: Impact on Land Management*; CRC Press: Boca Raton, FL, USA, 2008.
71. Wiegand, L.; Rhoades, J.D.; Escobar, D.E.; Everitt, J.H. Photographic and videographic observations for determining and mapping the response of cotton to soil salinity. *Remote Sens. Environ.* **1994**, *49*, 212–223. [[CrossRef](#)]
72. Chen, G.; Chen, Z.; Kamruzzaman, M. Monitoring of Wildlife Suitability Habitat Changes in Nature Reserves. *Rev. Cient. Fac. Cienc. Vet. Univ.* **2019**, *29*, 991–999.